ELSEVIER

Biochimica et Biophysica Acta 1514 (2001) 1–13

BIOCHIMICA ET BIOPHYSICA ACTA
BBA

www.bba-direct.com

Programmable fusogenic vesicles for intracellular delivery of antisense oligodeoxynucleotides: enhanced cellular uptake and biological effects

Qiang Hu [a,*], Clifford R. Shew [a], Marcel B. Bally [b], Thomas D. Madden [a,c]

[a] *Department of Pharmacology and Therapeutics, University of British Columbia, 2176 Health Sciences Mall, Vancouver, BC, Canada V6T 1Z3*

[b] *Division of Medical Oncology-Advanced Therapeutics, British Columbia Cancer Agency, 600 West 10th Avenue, Vancouver, BC, Canada V5Z 4E6*

[c] *Inex Pharmaceuticals Corporation, Burnaby, BC, Canada V5J 5JB*

Received 7 June 2000; received in revised form 30 January 2001; accepted 2 February 2001

Abstract

Programmable fusogenic vesicles (PFV) are liposomes composed of non-bilayer lipid components stabilized by the inclusion of an exchangeable poly(ethylene glycol) (PEG)-lipid conjugate. Vesicle destabilization by loss of the PEG-lipid results in recovery of the inherent fusogenic character. As a result, PFV can be designed to display a long circulation lifetime after i.v. administration, high accumulation at disease sites and full bioavailability of an encapsulated compound. In the present study, we investigated the potential application of PFV as carriers for intracellular delivery of antisense oligodeoxynucleotides (ODN). Antisense phosphorothioate ODN were encapsulated into PFV containing dioleoylphosphatidylethanolamine, cholesterol, dioleyldimethylammonium chloride and PEG-ceramides with different carbon chain length (C_8, C_{14} and C_{20}). In vitro fluorescent microscopy and flow cytometry analysis demonstrated that PFV containing PEG-ceramide C_{14} provided enhanced intracellular delivery of FITC-labelled antisense ODN compared to PFV displaying faster or slower rates of destabilization (containing PEG-ceramide C_8 or C_{20}, respectively). Therapeutic efficacy of PFV-encapsulated antisense ODN against two proto-oncogenes, c-*myc* and *bcl*-2, was examined in various cell lines. At antisense concentrations of 0.5 μM, no significant downregulation of c-*myc* mRNA levels was observed in HEK293, B16 and MCA207 cells. However, treatment of 518A2 melanoma cells with PFV-encapsulated antisense targeting *bcl*-2 at concentrations of 0.5 μM and 1.0 μM resulted in reduced *bcl*-2 mRNA level by about 20% and 25% after 48 h incubation. Free antisense ODN did not affect *bcl*-2 mRNA expression at the concentrations used in this study and encapsulated control antisense (reverse polarity) led to a non-specific increase in mRNA levels. Our results suggest that PFV carriers displaying appropriate rates of destabilization have the potential to act as intracellular delivery vehicles and may improve the bioavailability and potency of antisense oligonucleotides.

Keywords: Programmable fusogenic vesicle; Antisense; c-*myc*; *bcl*-2; Liposome

Abbreviations: EGFR, epidermal growth factor receptor; FITC, fluorescein isothiocyanate; HBS, HEPES buffered saline; HEPES, 4-(2-hydroxyethyl)-1-piperazineethanesulphonic acid; ODN, oligodeoxynucleotide(s); PBS, phosphate-buffered saline; PFV, programmable fusogenic vesicle(s); RT-PCR, reverse transcription-polymerase chain reaction

* Corresponding author. Fax: 604-822-4843. *E-mail address:* qiangh@interchange.ubc.ca (Q. Hu).

0005-2736/01/$ – see front matter
PII: S0005-2736(01)00294-2

1. Introduction

Antisense oligonucleotides are single-stranded, synthetic DNA sequences designed to be complementary to a specific gene. Hybridization with target pre-mRNA or mRNA through Watson–Crick base-pairing can activate RNase H-mediated degradation of the RNA strand in RNA–DNA heteroduplexes and subsequently inhibit gene expression at both mRNA and protein levels [1–4]. Since the earliest attempts by Zamecnik and Stephenson [5,6], antisense as a potential therapeutic agent against neoplastic and infectious diseases has been tested in numerous research laboratories around the world. Although one antisense drug received marketing approval in 1998 and several antisense compounds are in clinical trials [7], much of the preclinical work in this area has not been translated into therapeutic applications. One of the major obstacles to broad application of antisense technology is related to intracellular delivery. Fundamentally, these large polar molecules are unsuited to passive diffusion across cell membranes in their 'naked' form [8]. Even if they make their entrance into cells through fluid-phase pinocytosis or receptor-mediated endocytosis, internalized antisense oligodeoxynucleotides (ODN) remain mostly within vacuoles [9]. To compensate for this poor intracellular delivery, high doses are usually needed to achieve desirable therapeutic activities; however, these may trigger an acute toxicity response associated with high plasma ODN concentrations. In addition, external antisense can interact with cell surface proteins and interfere with normal cellular function in a non-sequence specific manner [10].

These problems with intracellular availability of free antisense have prompted studies into the development of carrier systems to enhance cellular uptake of antisense. Liposomes have been widely used in pharmaceutical applications as a delivery system for drugs and other bioactive molecules. These lipid vesicles are biodegradable, non-immunogenic, and able to encapsulate a wide variety of therapeutic agents. For antisense delivery, cationic liposomes have been widely used. These liposomes contain a cationic lipid, for DNA binding, and a non-bilayer-forming lipid to promote fusion with the plasma membrane. While cationic liposome–ODN complex system can work well in vitro [11,12], they are inherently unstable and apt to fuse to each other or the nearest available cell. This severely limits their suitability for systemic application. Recent development in liposomal formulation technology has identified a new type of liposome, termed programmable fusogenic vesicles (PFV) [13]. These liposomes contain cholesterol, charged lipid dioleyldimethylammonium chloride, and non-bilayer-forming lipid dioleoylphosphatidylethanolamine, stabilized by exchangeable poly(ethylene glycol) (PEG)-lipid conjugates [14]. They are initially stable in the circulation and protected from rapid clearance by the reticuloendothelial system (RES) as a result of the hydrophilic polymer coating. They can be designed to exhibit a long circulation time, allowing for accumulation at disease sites [15]. Upon loss of the PEG-lipid conjugates, which can be varied from minutes to hours, these vesicles become unstable and fusogenic [14]. In previous studies, PFV have shown promising anticancer drug delivery potential [16].

In the current study, we evaluated PFV as a delivery system for antisense molecules. The delivery of encapsulated antisense was characterized in different PFV formulations and compared to free antisense. The biological effects of antisense constructs designed against the proto-oncogenes, c-*myc* and *bcl*-2, were examined. The results reported in this study demonstrate that PFV systems with optimized rates of destabilization are promising delivery vehicles for antisense ODN.

2. Materials and methods

2.1. Materials

1,2-*sn*-Dioleoylphosphatidylethanolamine (DOPE) was purchased from Avanti Polar Lipids (Alabaster, AL). *N*,*N*-Dioleyl-*N*,*N*-dimethyl ammonium chloride (DODAC) and monomethoxypolyethylene$_{2000}$glycol succinate-($C_{8:0}$, $C_{14:0}$ or $C_{20:0}$ ceramide) (PEG-C_8, C_{14} or C_{20}) were kindly provided by Inex Pharmaceuticals (Vancouver, Canada). [^{3}H]Cholesteryl hexadecyl ether ([^{3}H]CHE) was bought from NEN Life Science (Boston, MA). Cholesterol, HEPES, sodium thiocyanate (NaSCN), and DEAE-Sepharose CL-6B were purchased from Sigma (Oakville, ON). Dialysis tubing (SpectraPor 12,000 to 14,000 mwco) was ob-

tained from Fisher Scientific (Ottawa, ON). Media and fetal calf serum for cell cultures, Trizol reagent, M-MLV reverse transcriptase, random hexamers and *Taq* DNA polymerase were originally obtained from Gibco BRL-Life Technologies (Burlington, ON). Propidium iodine was bought from Molecular Probes (Eugene, OR). Antisense c-*myc* (AS), fluorescein isothiocyanate (FITC)-epidermal growth factor receptor (EGFR) and mismatched control ODN (SAS) were the generous gifts from Inex Pharmaceuticals. Antisense *bcl*-2 (G3139, AS) and reverse-polarity control ODN (G3622, RP) were originally synthesized by Genta (Lexington, MA).

2.2. Cell lines and cell culture

Four different cell lines were investigated in gene regulation studies: HEK293, B16, MCA207 and 518A2. The human embryonic kidney cell line HEK293 and murine melanoma cell line B16 were obtained from ATCC and maintained in Dulbecco's modified Eagle's medium (HEK293) or minimum essential medium (B16). Chemically induced murine fibrosarcoma MCA207 cells were obtained from Dr. P. Joshi (Inex Pharmaceuticals, Vancouver, Canada) and maintained in RPMI 1640 medium. Human melanoma 518A2 cells were obtained from the British Columbia Cancer Agency and cultured in DMEM. All cells were grown in their designated medium supplemented with 10% fetal calf serum at 37°C in 5% CO_2. In addition, 2 mM L-glutamine was supplemented to B16 and MCA207 cells and 1 mM sodium pyruvate to B16 cells. For typical antisense delivery and gene regulation experiments, cells were seeded on 25 cm^2 Nunclon tissue culture flasks (Nunc, Roskilde, Denmark). In all experiments, cells were seeded 18–20 h prior to the treatment.

2.3. Antisense and control ODN

Both antisense and control sequences were fully phosphorothioated single strand ODN. Antisense c-*myc* (5′-AAC GTT GAG GGG CAT-3′) was complementary to the first five translation start codons of the human c-*myc* mRNA and the control ODN (5′-T AAG CAT ACG GGG TGT-3′) was a 16-mer mismatched sequence that preserved the G-quartet motif. Antisense *bcl*-2 (5′-TCT CCC AGC GTG CGC CAT-3′) was complementary to the first six translation start codons of the human *bcl*-2 mRNA and the control ODN for this antisense (5′-TAC CGC GTG CGA CCC TCT-3′) had the same sequence as that of the antisense but in a reverse-polarity arrangement. A 15-mer, five-prime FITC-labelled antisense to the gene stop codon of EGFR, FITC-EGFR, (5′-CCG TGG TCA TGC TCC-3′) was used to characterize the efficacy of in vitro delivery of ODN into cells.

2.4. PFV preparation and encapsulation of antisense ODN

Both antisense and control ODN were encapsulated within PFV based on an electrostatic interaction between the cationic lipid DODAC and the negative charges on the ODN phosphate groups. Briefly, DOPE, cholesterol, DODAC and PEG-ceramide (C_8, C_{14} or C_{20}) were dissolved in 100% ethanol at molar ratios of 35:45:15:5. Trace amounts of [^{3}H]CHE (approx. 0.01 μCi/mg lipid) were included in the mixture as a lipid marker. The lipid mixture (50 mM) was added to an aqueous solution of antisense (1 mg/ml) in 200 mM NaCl buffered with 20 mM HEPES, pH 7.4 (HBS) such that the final antisense:lipid ratio was 0.07:1 (w/w) and the final ethanol concentration was 30%. The vesicles were subsequently extruded through 100 nm pore size polycarbonate filters to create unilamellar vesicles using an Extruder (Lipex Biomembranes, Vancouver, BC) [17]. Ethanol was removed by dialysing the vesicles against HBS overnight at room temperature. Free and externally bounded antisense were removed by dialysis against 150 mM NaCl, 50 mM NaSCN, 20 mM HEPES, pH 7.4 for 5 h followed by ion exchange chromatography (DEAE-Sepharose CL-6B). The final antisense:lipid ratio in loaded PFV was approx. 0.03–0.04:1 (w/w) and the encapsulation efficiency of the PFV was in the range of 43–57%. The mean diameter of antisense loaded PFV ranged from 100 to 120 nm as determined by quasi-elastic light scattering using a Nicomp Model 270 particle sizer. Vesicles for cell culture studies were sterilized by terminal filtration through a 0.2 μm HT Tuffryn membrane filter (Gelman Science, Ann Arbor, MI).

2.5. Preparation of cationic liposome–ODN complexes

Cationic liposomes were prepared using a standard procedure. Briefly, DOPE and DODAC were dissolved in benzene:methanol (95:5, v/v) at the molar ratio of 50:50. The lipid mixture was lyophilized and subsequently hydrated in distilled H_2O. Vesicles were prepared by extrusion through 100 nm pore size polycarbonate filters after freeze and thawing cycles [18].

Preformed cationic liposomes were mixed with ODN in sterile water and incubated at room temperature for 30 min before adding to the cells. The concentrations of total lipid and ODN in the complex preparation were adjusted according to the desired charge ratio. In this study, the final charge ratio of cationic lipids:ODN was 1.3:1 (+:−) for *bcl*-2 antisense and 1.5:1 for c-*myc*.

2.6. In vitro antisense delivery studies and flow cytometry analysis

All intracellular delivery studies were carried out with HEK293 cells. In a typical experiment, free FITC-EGFR, empty PFV, or FITC-EGFR-loaded PFV were added to the cells (5×10^5 cells/flask), yielding a final antisense concentration of 0.2 μM. At various time points (0, 1, 2 or 4 h), cells were trypsinized, pelleted, washed and resuspended in phosphate-buffered saline (PBS). Cell-associated FITC fluorescent intensity was analysed using a FACSort dual-laser flow cytometer (Becton Dickinson, San Jose, CA). Propidium iodide (PI) was added to the cell suspension (1 μg/ml) prior to the reading as an indicator for cell membrane permeability. FITC and PI were detected in channel one (FL1, $\lambda_{em} = 530 \pm 15$ nm) and channel two (FL2, $\lambda_{em} = 585 \pm 21$ nm), respectively. A minimum of 10 000 events was collected for each sample. The data were analysed using CellQuest software (Becton-Dickinson). Antisense delivery and cellular compartmentalization were further assessed by fluorescent microscopy using a Zeiss Axiovert S100 inverted microscope equipped with an epifluorescence attachment. Photographs were taken using Kodak Ektachrome P1600 film.

2.7. Downregulation of c-myc and bcl-2 mRNA using free antisense, antisense–liposome complexes or PFV-encapsulated antisense

Cells were cultured in 25 cm^2 flasks at an initial density of 5×10^5 cells/flask. Antisense was delivered either as free ODN, by cationic liposome complexes, or by PFV. The control cells were treated with the same volume of HBS (PFV delivery) or distilled H_2O (liposome complex delivery). Using antisense–liposome complexes, cells were treated in a serum-free culture environment. Cells were incubated in serum-free media either up to the time point (≤ 8 h) or for 4 h after which the media were replaced with serum-containing media for longer time points (24 h). In the case of antisense delivery using PFV, cells were maintained in serum-containing media. At various time points (4, 8, 24 or 48 h), media were removed and cells were directly lysed in the flask. Total RNA was extracted using Trizol reagent following the manufacturer's instructions.

Quantitation of c-*myc* and *bcl*-2 mRNA levels was carried out using reverse transcription-polymerase chain reaction (RT-PCR) following a standard pro-

Table 1
Primers used for PCR amplification and expected length of DNA fragment

Gene	Primer pair	Product size (bp)
bcl-2 (human)	5′-ATGGCGCACGCTGGGAGAAC-3′	327
	5′-GCGGTAGCGGCGGGAGAAGT-3′	
c-*myc* (human)	5′-TAATTCCAGCGAGAGGCAGAGG-3′	618
	5′-ACGTAGGAGGGCGAGCAGAG-3′	
c-*myc* (mouse)	5′-CGCTGGGAAACTTTGCCCAT-3′	492
	5′-CGCCGTCATCGTCTTCCCTT-3′	
β-actin	5′-TGATCCACATCTGCTGGAAGGTGG-3′	524 (human)
	5′-GGACCTGACTGACTACCTCATGAA-3′	523 (mouse)

cedure [19]. Briefly, first strand cDNA was synthesized from 2.5 μg total RNA using M-MLV reverse transcriptase and random hexamers in 50 mM Tris–HCl (pH 8.3), 75 mM KCl, 10 mM DTT, and 2 mM dNTPs. The reaction was allowed to proceed for 1 h at 37°C and stopped by incubation of reaction mixture at 95°C for 5 min. Reverse transcription reaction products subsequently underwent PCR amplification for the detection of specific genes. Aliquots (3 μl) of RT reaction products were amplified separately for *bcl*-2, c-*myc* and β-actin (internal standard) by PCR in 20 mM Tris–HCl (pH 8.4), 50 mM KCl, 1.5 mM $MgCl_2$, 0.8 mM dNTPs, 0.25 μM each of the gene specific primers and 1.5 U of *Taq* DNA polymerase. The primers for each specific gene and the sizes of amplification products are listed in Table 1. DNA amplification was performed using a Perkin-Elmer DNA thermocycler under the following conditions: 30 s at 94°C followed by 1.5 min at 65°C for 20–35 cycles. Appropriate cycle numbers were determined experimentally for each of the interested genes in each cell line. Amplified products (10 μl) were electrophoresed in 1.5% (w/v) agarose gel stained by ethidium bromide. Levels of relative band intensity, corrected on the basis of β-actin level, were quantitated using a digital camera (Eagle Eye II, Stratagene) coupling with ImageQuant software (Molecular Dynamic, CA). The final values of c-*myc* or *bcl*-2 mRNA abundance were expressed as percentages of the untreated control cells.

2.8. Statistical analysis

Data from gene regulation studies were evaluated with one-way ANOVA using SigmaStat software. Differences among treatment groups were further evaluated with the Student–Newman–Keuls test. A statistically significant difference was reported if $P < 0.05$.

3. Results

3.1. Delivery of FITC-labelled antisense to HEK293 cells: free and PFV-encapsulated ODN

The ability of PFV to deliver antisense molecules efficiently to HEK293 cells was examined using flow cytometry. FITC-labelled antisense (EGFR) was introduced to the cell medium as the free oligonucleotide, in the presence of empty PFV, or encapsulated in PFV containing PEG-ceramide C_{14}. As shown in Fig. 1, cells treated with free antisense demonstrated little or no uptake. The mean fluorescence in these cells was not significantly different from that in control cells. In contrast, at the same antisense concentration (0.2 μM), cells incubated with PFV-encapsulated antisense exhibited efficient accumulation of FITC-EGFR, to levels 20 times higher than obtained for free antisense. As can be seen, cellular uptake of free antisense was also enhanced in the presence of empty PFV, but not to the same level seen for encapsulated ODN. Destabilization of PFV through exchange of PEG-lipid conjugates will expose the cationic surface. Binding of free antisense may then occur with subsequent introduction of this antisense into cells either through fusion of the complex with the plasma membrane [20–22] or by complex endocytosis [23,24]. Nevertheless, the most effective delivery of antisense was achieved for PFV-encapsulated ODN.

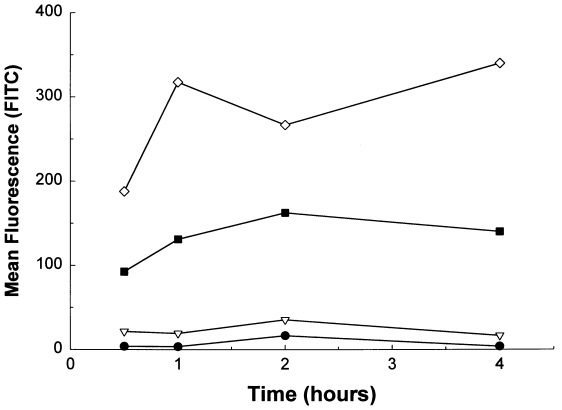

Fig. 1. Time course of FITC-labelled antisense uptake, displayed as mean fluorescence, by HEK293 cells upon exposure to free antisense (▽), free antisense plus empty PFV (■) and PFV encapsulated antisense (◇). Untreated cells were presented as the control (●).

3.2. Influence of PEG-ceramide acyl chain length on PFV-mediated delivery of antisense

The rate of PFV destabilization is governed by the exchange rate of the PEG-ceramide component. In turn, this rate is determined by the ceramide *N*-acyl chain length which 'anchors' the conjugate within the

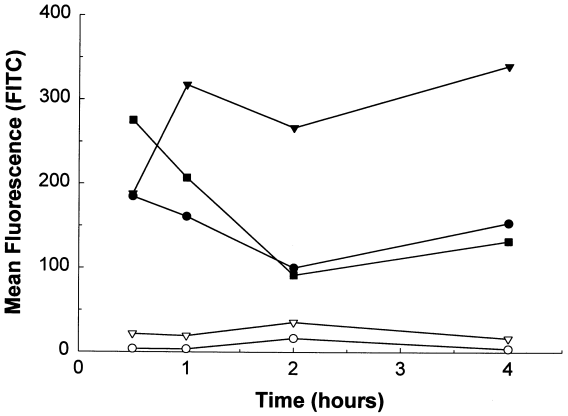

Fig. 2. Influence of PEG-ceramide acyl chain length on cellular uptake of FITC-labelled antisense by HEK293 cells. Antisense was delivered as free antisense (▽), by PFV containing PEG-ceramide C_8 (●), PEG-ceramide C_{14} (▼), or PEG-ceramide C_{20} (■). Untreated cells were presented as control (○).

lipid bilayer. As the *N*-acyl chain is shortened, the rate of lipid exchange and vesicle destabilization increases [25]. To evaluate the influence of *N*-acyl chain length on delivery of antisense molecules in vitro, we examined PFV systems containing PEG-ceramide of varying *N*-acyl chain length, i.e., C_8, C_{14}, or C_{20}, respectively. As shown in Fig. 2, for all three PFV formulations the intensity of mean fluorescence in cells was elevated compared to free antisense. Significant differences were seen, however, in the time course and magnitude of ODN delivery for the different PFV formulations. When antisense was delivered by PFV containing PEG-ceramide C_{14}, cell-associated fluorescence intensity increased steadily over 4 h. In contrast, when antisense was delivered by PFV containing PEG-ceramide C_8 or C_{20}, cell-associated fluorescence intensity exhibited an initial jump, similar to that seen for the PEG-ceramide C_{14} formulation, followed by a decline over 4 h. After 4 h, the highest mean fluorescence was observed in cells treated with PFV containing PEG-ceramide C_{14}, which was about twice as high as samples incubated with PFV containing PEG-ceramide C_8 or C_{20}.

3.3. Antisense intracellular compartmentalization following delivery by PFV with PEG-ceramides of varying N-acyl chain length

Flow cytometry provides information on FITC-ODN association with cells but does not allow determination of intracellular distribution. We therefore examined cells after incubation with free or PFV-encapsulated ODN by fluorescence microscopy. As for the flow cytometry studies, HEK293 cells were incubated with antisense encapsulated in PFV containing PEG-ceramides of varying *N*-acyl chain length. After 4 h incubation, cells were washed with PBS and observed under phase contrast and fluorescence microscopy. Significant differences in the cellular distribution of FITC-labelled antisense, as a function of PFV composition, were apparent (Fig. 3). In the case of PFV containing PEG-ceramide C_8 (Fig. 3A,B), fluorescence microscopy revealed a punctate distribution of FITC-ODN predominantly distributed around the cell surface. No significant intracellular fluorescence was seen. In contrast, FITC-EGFR delivered using PFV containing PEG-ceramide C_{14} (Fig. 3C,D) was predominantly internalized, exhibiting diffuse fluorescence, mainly in the cytoplasm. In the case of PFV containing PEG-ceramide C_{20} (Fig. 3E,F), fluorescence was mainly observed on the cell surface. This pattern was similar to that observed for PFV containing PEG-ceramide C_8; however, the FITC-EGFR distribution was somewhat less punctate. These observations are consistent with the rate of vesicle destabilization governing the efficiency of antisense internalization. In light of the fluorescence microscopy results it appears likely that the initial increase in cell-associated fluorescence seen by flow cytometry (Fig. 2) represents surface-absorbed PFV and not internalized antisense, particularly in the case of formulation containing PEG-ceramides with C_8 and C_{20} *N*-acyl chain lengths.

3.4. Antisense effects on c-myc mRNA expression

Based on the fluorescence microscopy studies, it is clear that antisense molecules can be effectively delivered into cells using PFV formulations incorporating PEG-ceramide C_{14}. The next question addressed concerned the subsequent biological effects of antisense ODN on target genes. This was first investigated using a 15-mer antisense construct targeting the proto-oncogene c-*myc*. This antisense construct has been shown previously to inhibit c-*myc* protein expression and cell proliferation of human leukaemic cell line HL-60 [26]. Antitumour effects are also dem-

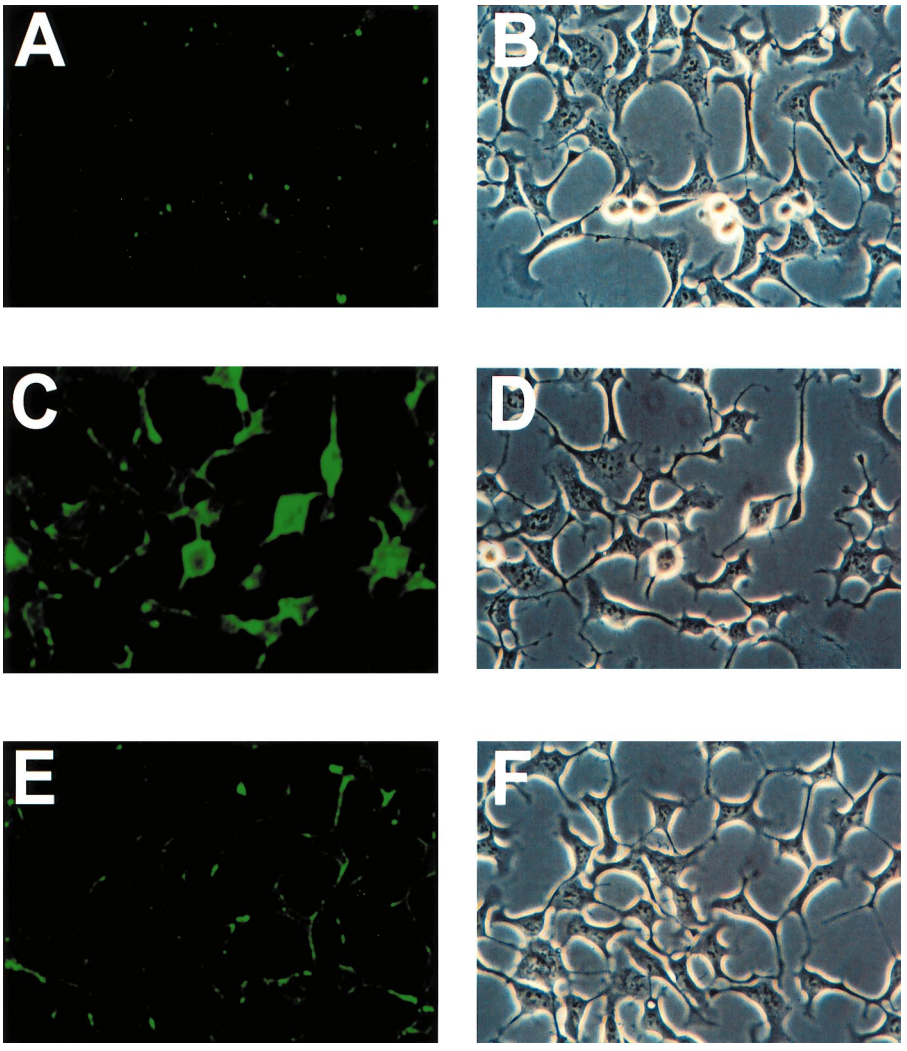

Fig. 3. Intracellular localization of FITC-labelled antisense in HEK293 cells after 4 h incubation. Antisense was delivered by PFV containing PEG-ceramide C_8 (A,B), PEG-ceramide C_{14} (C,D), or PEG-ceramide C_{20} (E,F).

onstrated in several animal models [27–29]. We examined the antisense effects on three cell lines: in addition to HEK293 cells, two mouse tumour cell lines were investigated for comparison. As described in Section 2, free antisense, empty PFV, PFV-encapsulated control ODN (SAS), or PFV-encapsulated antisense ODN (AS) were introduced to cells at a final ODN concentration of 0.5 μM (or equivalent PFV concentration). Levels of c-*myc* mRNA were analysed after 4, 8, 24, or 48 h incubation. Empty PFV were used to monitor possible changes in gene expression in cells responding to cationic lipids. Levels of mRNA, standardized against β-actin, are shown in Fig. 4. Despite the efficient cellular delivery previously demonstrated, no clear antisense effects at the mRNA level were seen for any of the cell lines studied over 48 h. It appeared that after 24 h treatment with encapsulated antisense ODN, both HEK293 and B16 cells showed a slight reduction in mRNA abundance compared to free antisense and control ODN treatments (Fig. 4A,B). However, this reduction was not statistically significant. We also observed non-specific stimulation of mRNA levels when cells were exposed to both ODN and liposomes. This was seen in all of the cell lines treated with control ODN after 24 h incubation. The mechanism for this upregulation effect is not clear. However, this might partially mask or offset an antisense-

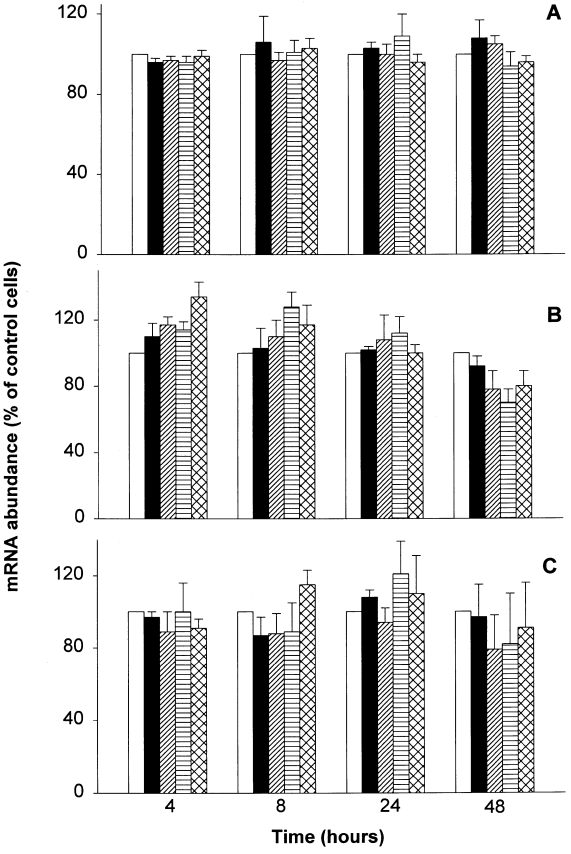

Fig. 4. Expression of c-*myc* mRNA in HEK293 cells (A), B16 cells (B) and MCA207 cells (C) upon exposure to HBS (control, open bar), free antisense (shaded), empty PFV (diagonal hatched), PFV-encapsulated control ODN (SAS) (horizontal hatched), or PFV-encapsulated antisense (AS) (cross-hatched). The abundance of c-*myc* mRNA was quantified by RT-PCR as described in Section 2. Values are presented as means ± S.E.M. ($n = 2$).

mediated reduction. It is also possible that the encapsulated antisense was not completely bioavailable to the target genes. To test this possibility, we carried out another set of experiments using cationic liposome–ODN complexes for delivery [20,30]. Free antisense, cationic liposome, control ODN–liposome complexes, or antisense–liposome complexes were added to HEK293 cells or B16 cells at the same ODN concentration as that of PFV delivery. Downregulation of c-*myc* mRNA was evaluated after 2, 4, or 8 h treatment. As shown in Fig. 5, downregulation was seen with B16 cells after 4 and 8 h incubation, but this represented a maximum decrease of only about 20% relative to free antisense and control cells. Downregulation of c-*myc* mRNA was also exhibited with HEK293 cells after 2 h treatment. However, this might not be a true antisense effect because a similar decrease in mRNA level was displayed by cells treated with cationic liposomes alone. It has been suggested that the target gene reduction may be attributed to the toxicity of cationic liposome complexes instead of a true antisense effect [31]. Results from our cell toxicity studies, however, indicated a reciprocal relationship between cell viability and c-*myc* expression. Upon exposing cells to cationic liposomes or liposome–ODN complexes for 4 or 8 h, both HEK293 and B16 cells exhibited varied levels of cytotoxic effect. Severe cytotoxicity (50–60% reduction of cell viability) was displayed in cells that were treated with liposome–ODN complexes (data not shown). Corresponding to the reduction of viability, all cells, except the B16 cells treated with antisense–liposome complexes, exhibited elevated c-*myc* mRNA expression compared to the control cells (Fig. 5). Our data showed that with similar levels of cytotoxic effect among different treatments, or higher in the case of control ODN–liposome com-

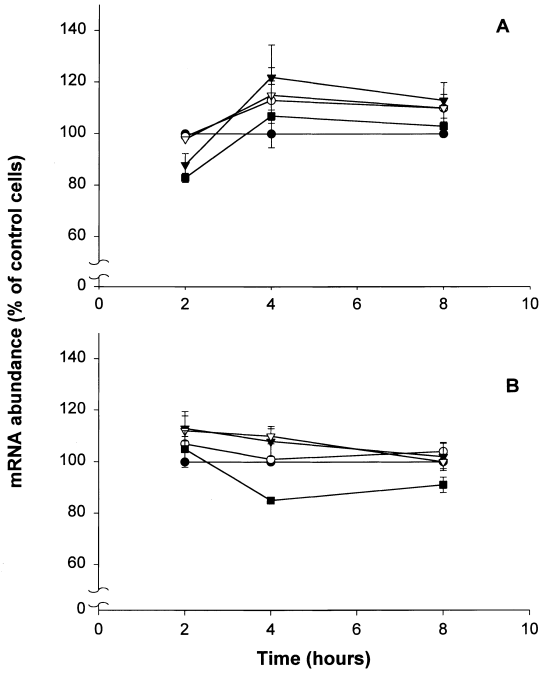

Fig. 5. Expression of c-*myc* mRNA in HEK293 cells (A) and B16 cells (B) upon exposure to free antisense (○), cationic liposome (▼), control ODN–liposome complexes (SAS-C) (▽), or antisense ODN–liposome complexes (AS-C) (■). Control cells (●) were treated with an equal volume of distilled water. Values are presented as means ± S.E.M. ($n = 2$).

plexes, only cells treated with antisense–liposome complexes displayed target gene reduction. This seems to suggest that the downregulation effect of c-*myc* antisense observed under our experimental conditions is not a direct cause of cytotoxicity. The most striking observation from the cationic liposome complex delivery studies is the reciprocal relationship between cell viability and c-*myc* expression. It is possible that the c-*myc* is overexpressed to compensate the cell death induced by liposomal complexes. The mechanism for this upregulation of c-*myc* mRNA has not been fully understood. In summary, no consistent or significant reduction in c-*myc* mRNA level was seen for antisense delivered using either cationic liposome complexes or PFV.

3.5. Antisense effects on bcl-2 mRNA expression

The inability to demonstrate downregulation of c-*myc* mRNA levels might reflect the binding affinity of the ODN construct for its complementary sequence, or rapid turnover of c-*myc* mRNA. To further investigate the efficacy of the PFV delivery system, we therefore studied an 18-mer antisense construct against the proto-oncogene *bcl*-2. In previous studies, this antisense has been proved a potent therapeutic agent. When delivered by cationic liposome complexes, this antisense has successfully inhibited gene expression at both mRNA and protein levels and prevented cell growth by inducing apoptosis in human melanoma cell lines (including 518A2) [32]. Our preliminary experiments on 518A2 cells confirmed that *bcl*-2 mRNA expression was significantly reduced after exposure to antisense–liposome complexes for 24 h. This reduction also appeared to be ODN concentration dependent (data not shown). Further examination indicated that the downregulation effect was antisense specific. As shown in Fig. 6, exposing 518A2 cells to antisense–cationic liposome complexes at a final ODN concentration of 0.5 μM, *bcl*-2 mRNA levels were reduced by 60% after 24 h incubation. The reverse polarity control ODN (RP) produced less than 30% reduction in message levels. Using this antisense construct and the 518A2 cell line, we examined the PFV delivery system. Cells were exposed to free antisense, empty PFV, PFV-encapsulated control RP, or PFV-encapsulated AS for 24 or 48 h at two antisense concentrations: 0.5 μM and 1.0 μM. The level of mRNA expression under different treatments is illustrated in Fig. 7 and the numerical results are shown in Fig. 8. An antisense specific downregulation effect was clearly observed after 48 h treatment by antisense encapsulated in PFV at both concentrations. With PFV delivery, mRNA expression in cells was reduced, relative to the control cells, by about 20% at an antisense concentration of 0.5 μM (Fig. 8A). In the case of cells treated with PFV containing the control, reverse po-

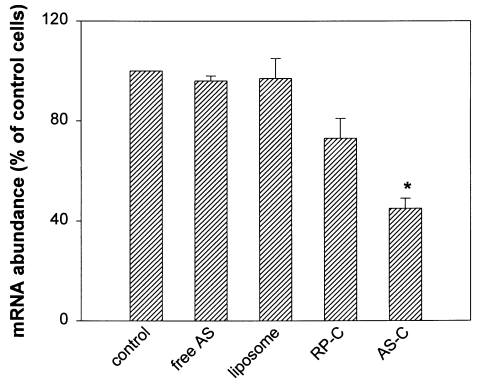

Fig. 6. Expression of *bcl*-2 mRNA in 518A2 cells upon exposure to free antisense, cationic liposome, control ODN–liposome complexes (RP-C), or antisense–liposome complexes (AS-C) for 24 h at a final antisense ODN concentration of 0.5 μM. Control cells were treated with an equal volume of distilled water. The abundance of *bcl*-2 mRNA was quantified by RT-PCR. Values are presented as means ± S.E.M. ($n = 4$). *Significant difference between AS-C and the rest of the treatment groups ($P < 0.05$).

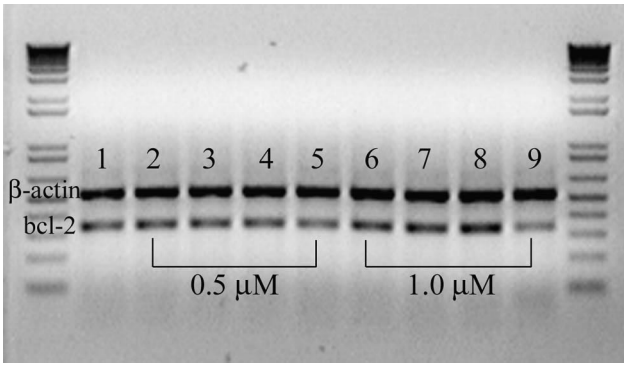

Fig. 7. Representative RT-PCR analysis of *bcl*-2 mRNA expression in 518A2 cells after 48 h exposure to HBS (lane 1), free antisense (lanes 2 and 6), empty PFV (lanes 3 and 7), PFV-encapsulated control ODN (lanes 4 and 8), or PFV-encapsulated antisense ODN (lanes 5 and 9). The final antisense concentration is 0.5 μM (lanes 2–5) or 1.0 μM (lanes 6–9), respectively.

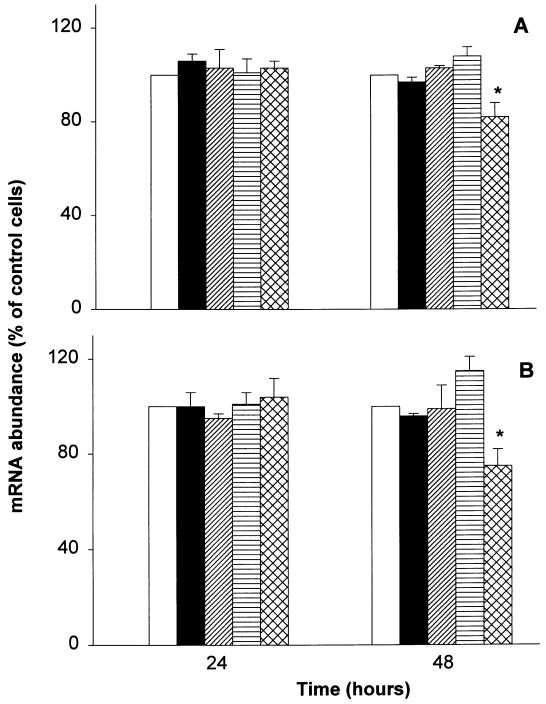

Fig. 8. Expression of *bcl*-2 mRNA in 518A2 cells upon exposure to HBS (control, open bar), free antisense (shaded), empty PFV (diagonal hatched), PFV-encapsulated control ODN (RP) (horizontal hatched), or PFV-encapsulated antisense ODN (AS) (cross-hatched) at a final antisense concentration of 0.5 μM (A) or 1.0 μM (B). Values are presented as means ± S.E.M. ($n = 3$–5). *Significant difference between AS-loaded PFV and RP-loaded PFV ($P < 0.05$).

larity, ODN, an upregulation of *bcl*-2 mRNA was seen. Compared to this control ODN, therefore, the reduction of mRNA expression in cells treated with PFV-encapsulated antisense was about 30%. When the antisense concentration was increased to 1.0 μM, the mRNA level was further reduced, by about 25% compared to the control cells (Fig. 8B). However, cells treated with PFV containing the control ODN showed an even higher stimulation on mRNA expression. The difference in mRNA levels between antisense versus control ODN was therefore about 40%. It was also apparent from Fig. 8 that a lag period existed between initial treatment of cells with *bcl*-2 antisense in PFV, and message downregulation. This lag period was not seen when antisense was delivered using cationic liposome complexes. This delay also appeared to be independent of antisense concentration. Further in contrast to the results obtained with cationic liposome complexes, delivery of control, reverse polarity ODN in PFV did not result in a non-sequence specific reduction in mRNA.

4. Discussion

For many applications, an 'ideal' drug delivery carrier should possess the following properties: it should be stable and remain in the circulation system long enough to allow maximum accumulation at the disease site; once reaching the site, it should become fusogenic or 'leaky' making encapsulated drugs bioavailable to the target cells. Conventional liposomal carriers that exhibit long circulation lifetime and high disease site deposition are designed to be physically stable and resistant to leakage or fusion. As a result encapsulated drugs may not be adequately released from the carriers even after they have accumulated at the target sites. For a stable liposome to become leaky requires an intrinsic change to its biophysical or structural properties. In programmable fusogenic vesicles, this is achieved by using non-lamellar-forming lipids, DOPE, which in isolation adapt the hexagonal H_{II} phase, cholesterol and DODAC. This mixture is stabilized in a bilayer organization only by the presence of an exchangeable component, PEG-lipid [14]. The PEG-lipid component can also inhibit protein binding, and subsequent vesicle clearance, after intravenous administration of PFV [33–35]. As a consequence of their hydrophilic polymer chain, however, PEG-lipids, such as PEG-ceramide, can desorb from the PFV membrane and exchange to other hydrophobic binding sites [36]. Gradually, with loss of PEG-ceramide, the initially stable PFV will be destabilized resulting in either fusion to an adjacent membrane and/or release of encapsulated compounds [13,14,37]. An important factor in designing an efficient carrier system is to control the rate of vesicle destabilization. If the vesicles destabilize in the circulation, accumulation at the disease site will be compromised. The rate of PFV destabilization is controlled by the PEG-lipid component. By varying the hydrophobic 'anchor' domain, one can modulate the fusion process over minutes to hours [25]. For the delivery of large polar molecules such as antisense ODN, PFV also need to interact directly with cell membranes. Simply releasing antisense in the vicinity of target cells, following PFV destabili-

zation, does not address the problem of uptake into the cell cytoplasm. The inclusion of a cationic lipid, DODAC, is therefore intended to promote the interaction between vesicles and cell membranes [38]. Subsequent fusion of the carrier with the plasma membrane, or an endosomal membrane following endocytosis, would provide an opportunity for the encapsulated oligonucleotide to be released directly into the cytoplasm.

The results reported in the current study demonstrate that antisense delivery and cell internalization can be achieved when the oligonucleotide is encapsulated in an optimized PFV. In vitro, cellular uptake of antisense is significantly enhanced when the PFV carrier undergoes destabilization over several hours i.e. for PFV containing PEG-ceramide C_{14} [13]. More importantly, with this delivery system, antisense can be largely delivered into the cell cytoplasm. When PFV destabilization occurs over much shorter or longer time periods, i.e. for systems containing PEG-ceramides C_8 and C_{20}, respectively, efficient intracellular delivery of antisense is not observed. In the case of PFV containing PEG-ceramide C_8, it is likely that rapid loss of the stabilizing component results in aggregation of the carriers before they can interact with the cell surface. In contrast, systems containing PEG-ceramide C_{20} would not be expected to destabilize over the time course of the experiment [25,36] and hence vesicle fusion or antisense release is not anticipated. It is important to note that an optimal PFV formulation for in vitro applications may not be the ideal candidate for in vivo use. Carrier accumulation at, for example, tumour sites is dependent on circulation lifetime in the blood [15] and hence a slower rate of destabilization may be required to maximize tumour loading.

After delivery into cells, antisense ODN can exert their biological activity through one of the following mechanisms: interrupting RNA interaction with ribosomes; blocking mRNA passage from nucleus to cytoplasm; hybridizing with the cytoplasmic target mRNA and resulting in the arrest of translation; and triggering cleavage of the hybridized mRNA by RNase H [39,40]. To achieve efficient downregulation of mRNA levels, it is suggested that RNase H enzymatic cleavage should be involved [41–43]. RNase H, a ubiquitous group of endonucleases that cleave the RNA strand in RNA–DNA heteroduplexes, is mainly located in the nucleus [44]. The level of RNase H and its activity vary between cell lines and are also dependent on antisense concentration [45]. The efficacy of RNase H cleavage of RNA–DNA hybrids depends on sequence binding affinity, which is antisense molecule specific [46]. Obviously, to get a maximum antisense effect, all three components, i.e. enzyme, antisense ODN and target mRNA, should be located in the same subcellular compartment. Currently, we do not completely understand the mechanism(s) by which antisense reaches the nucleus after being delivered into cells by liposomes. Previous studies have shown effective nuclear localization of antisense and downregulation of mRNA expression following delivery as cationic liposome complexes [32,47,48]. In our present study, therefore, cationic liposome–ODN complexes were used as a positive control in message downregulation studies. In the case of c-*myc* antisense, all tested cell lines were unresponsive to the antisense ODN at the concentration used. Even with cationic liposome complex delivery, message downregulation is minimal. We suggest that the poor biological effect detected for this antisense may be due to a poor RNase H enzyme activity, which is dependent upon both cellular and ODN factors. For antisense *bcl*-2, on the other hand, promising specific antisense effects are observed with both delivery systems. Compared to cationic liposome complex delivery, PFV systems require a longer period before mRNA downregulation is observed. This lag period may relate to the time required for PFV destabilization. When higher concentrations of *bcl*-2 antisense in PFV were administered to cells (1.0 μM compared to 0.5 μM) only a small additional decrease in mRNA level was observed. This may reflect saturation of binding sites of PEG-ceramide in vitro and hence decreased efficiency of vesicle destabilization. Additional experiments are undergoing to address this issue.

An important difference between the use of cationic liposome complexes and PFV is that serum interferes with antisense delivery using cationic complexes [49]. Accordingly, incubations must be performed in serum-free media. As illustrated in the present work, this is not a limitation for PFV and is clearly an important consideration for subsequent in vivo applications.

Acknowledgements

We would like to thank Dr. Jeff Hewitt for his assistance in PCR primer design, Inex Pharmaceutical Co. for providing some of the facilities, and two anonymous referees for their valuable suggestions. This work was supported by a grant from the National Cancer Institute of Canada through funds provided by the Canadian Cancer Society. (T.D.M. and M.B.B.).

References

[1] C. Helene, J.J. Toulme, Specific regulation of gene expression by antisense, sense and antigen nucleic acids, Biochim. Biophys. Acta 1049 (1990) 99–125.
[2] S.T. Crooke, Therapeutic applications of oligonucleotides, Annu. Rev. Pharmacol. Toxicol. 32 (1992) 329–376.
[3] C.A. Stein, Y.C. Cheng, Antisense oligonucleotides as therapeutic agents – Is the bullet really magical?, Science 261 (1993) 1004–1012.
[4] R.W. Wagner, Gene inhibition using antisense oligodeoxynucleotides, Nature 372 (1994) 333–335.
[5] P.C. Zamecnik, M.L. Stephenson, Inhibition of Rous sarcoma virus replication and cell transformation by a specific oligodeoxynucleotide, Proc. Natl. Acad. Sci. USA 75 (1978) 280–285.
[6] M.L. Stephenson, P.C. Zamecnik, Inhibition of Rous sarcoma virus RNA translation by a specific oligodeoxynucleotide, Proc. Natl. Acad. Sci. USA 75 (1978) 285–288.
[7] A. Persidis, Antisense therapeutics, Nat. Biotechnol. 17 (1999) 403–404.
[8] R.E. Clark, Poor cellular uptake of antisense oligodeoxynucleotides: an obstacle to their use in chronic myeloid leukaemia, Leuk. Lymphoma 19 (1995) 189–195.
[9] S. Akhtar, R.L. Juliano, Cellular uptake and intracellular fate of antisense oligonucleotides, Trends Cell Biol. 2 (1992) 139–144.
[10] P. Rockwell, W.J. O'Connor, K. King, N.I. Goldstein, L.M. Zhang, C.A. Stein, Cell-surface perturbations of the epidermal growth factor and vascular endothelial grow factor receptors by phosphorothioate oligodeoxynucleotides, Proc. Natl. Acad. Sci. USA 94 (1997) 6523–6528.
[11] S.A. Williams, L. Chang, J.S. Buzby, Y. Suen, M.S. Cairo, Cationic lipids reduce time and dose of c-myc antisense oligodeoxynucleotides required to specifically inhibit Burkitt's lymphoma cell growth, Leukemia 10 (1996) 1980–1989.
[12] G. Hartmann, A. Krug, M. Bidlingmaier, U. Hacker, A. Eigler, R. Albrecht, C.J. Strasburger, S. Endres, Spontaneous and cationic lipid-mediated uptake of antisense oligonucleotides in human monocytes and lymphocytes, J. Pharmacol. Exp. Ther. 285 (1998) 920–928.
[13] J.W. Holland, C. Hui, P.R. Cullis, T.D. Madden, Poly(ethylene glycol)-lipid conjugates regulate the calcium-induced fusion of liposomes composed of phosphatidylethanolamine and phosphatidylserine, Biochemistry 35 (1996) 2618–2624.
[14] J.W. Holland, P.R. Cullis, T.D. Madden, Poly(ethylene glycol)-lipid conjugates promote bilayer formation in mixtures of non-bilayer-forming lipids, Biochemistry 35 (1996) 2610–2617.
[15] A.A. Gabizon, Selective tumor localization and improved therapeutic index of anthracyclines encapsulated in long circulating liposomes, Cancer Res. 52 (1992) 891–896.
[16] G. Adlakha-Hutcheon, M.B. Bally, C.R. Shew, T.D. Madden, Controlled destabilization of a liposomal drug delivery system enhances mitoxantrone antitumor activity, Nat. Biotechnol. 17 (1999) 775–779.
[17] M.J. Hope, M.B. Bally, G. Webb, P.R. Cullis, Production of large unilamellar vesicles by a rapid extrusion procedure: characterization of size distribution, trapped volume and ability to maintain a membrane potential, Biochim. Biophys. Acta 852 (1985) 123–126.
[18] L.D. Mayer, M.J. Hope, P.R. Cullis, A.S. Janoff, Solute distributions and trapping efficiencies observed in freeze-thawed multilamellar vesicles, Biochim. Biophys. Acta 817 (1985) 193–196.
[19] J. Chelly, A. Kahn, RT-PCR and mRNA quantitation, in: K.B. Mullis, F. Ferré, R.A. Gibbs (Eds.), The Polymerase Chain Reaction, Birkhäuser, Boston, MA, 1994, pp. 97–109.
[20] P.L. Felgner, T.R. Gadek, M. Holm, R. Roman, H.W. Chan, M. Wenz, J.P. Northrop, G.M. Ringold, M. Danielsen, Lipofection: A highly efficient, lipid-mediated DNA-transfection procedure, Proc. Natl. Acad. Sci. USA 84 (1987) 7413–7417.
[21] L. Stamatatos, R. Leventis, M.J. Zuckermann, J.R. Silvius, Interactions of cationic lipid vesicles with negatively charged phospholipid vesicles and biological membranes, Biochemistry 27 (1988) 3917–3925.
[22] P. Pires, S. Simões, S. Nir, R. Gaspar, N. Düzgünes, M.C. Pedroso de Lima, Interaction of cationic liposomes and their DNA complexes with monocytic leukemia cells, Biochim. Biophys. Acta 1418 (1999) 71–84.
[23] H. Farhood, N. Serbina, L. Huang, The role of dioleoyl phosphatidylethanolamine in cationic liposome mediated gene transfer, Biochim. Biophys. Acta 1235 (1995) 289–295.
[24] I. Wrobel, D. Collins, Fusion of cationic liposomes with mammalian cells occurs after endocytosis, Biochim. Biophys. Acta 1235 (1995) 296–304.
[25] J.R. Silvius, R. Leventis, Spontaneous interbilayer transfer of phospholipids: dependence on acyl chain composition, Biochemistry 32 (1993) 13318–13326.
[26] R. Heikkila, G. Schwab, E. Wickstrom, S.L. Loke, D.H. Pluznik, R. Watt, L.M. Neckers, A c-myc antisense oligodeoxynucleotide inhibits entry into S phase but not progress from G_0 to G_1, Nature 328 (1987) 445–449.

[27] C. Leonetti, I. D'Agnano, F. Lozupone, A. Valentini, T. Geiser, G. Zon, B. Calabretta, G. Citro, G. Zupi, Antitumor effect of c-myc antisense phosphorothioate oligodeoxynucleotides on human melanoma cells in vitro and in vivo, J. Natl. Cancer Inst. 88 (1996) 419–429.
[28] T. Skorski, D. Perroti, M. Nieborowska-Skorska, S. Gryaznov, B. Calabretta, Antileukemia effect of c-myc N3′-P5′ phosphoramidate antisense oligonucleotides in vivo, Proc. Natl. Acad. Sci. USA 94 (1997) 3966–3971.
[29] E. Wickstrom, Antisense c-myc inhibition of lymphoma growth, Antisense Nucleic Acid Drug Dev. 7 (1997) 225–228.
[30] C.F. Bennett, M.Y. Chiang, H. Chan, J.E.E. Shoemaker, C.K. Mirabelli, Cationic lipids enhance cellular uptake and activity of phosphorothioate antisense oligonucleotides, Mol. Pharmacol. 41 (1992) 1023–1033.
[31] K. Konopka, J.J. Rossi, P. Swiderski, V.A. Slepushkin, N. Düzgünes, Delivery of an anti-HIV ribozyme into HIV-infected cells via cationic liposomes, Biochim. Biophys. Acta 1372 (1998) 55–68.
[32] B. Jansen, H. Schlagbauer-Wadl, B.D. Brown, R.N. Bryan, A. Van Elsas, M. Müller, K. Wolf, H.-G. Eichler, H. Pehamberger, bcl-2 antisense therapy chemosensitizes human melanoma in SCID mice, Nat. Med. 4 (1998) 232–234.
[33] D.D. Lasic, F.J. Martin, A. Gabizon, S.K. Huang, D. Papahadjopoulos, Sterically stabilized liposomes: a hypothesis on the molecular origin of the extended circulation times, Biochim. Biophys. Acta 1070 (1991) 187–192.
[34] J. Senior, C. Delgado, D. Fisher, C. Tilcock, G. Gregoriadis, Influence of surface hydrophilicity of liposomes on their interaction with plasma protein and clearance from the circulation: studies with poly(ethylene glycol)-coated vesicles, Biochim. Biophys. Acta 1062 (1991) 77–82.
[35] V.P. Torchilin, V.G. Omelyanenko, M.I. Papisov, A.A. Bogdanov, V.S. Trubetskoy, J.H. Herron, C.A. Gentry, Poly(ethylene glycol) on the liposome surface: on the mechanism of polymer-coated liposome longevity, Biochim. Biophys. Acta 1195 (1994) 11–20.
[36] J.R. Silvius, M.J. Zuckermann, Interbilayer transfer of phospholipid-anchored macromolecules via monomer diffusion, Biochemistry 32 (1993) 3153–3161.
[37] S.M. Gruner, Intrinsic curvature hypothesis for biomembrane lipid composition: a role for nonbilayer lipids, Proc. Natl. Acad. Sci. USA 82 (1985) 3665–3669.
[38] L. Stamatatos, R. Leventis, M.J. Zuckermann, J.R. Silvius, Interactions of cationic lipid vesicles with negatively charged phospholipid vesicles and biological membranes, Biochemistry 27 (1988) 3917–3925.
[39] A. Alama, F. Barbieri, M. Cagnoli, G. Schettini, Antisense oligonucleotides as therapeutic agents, Pharm. Res. 36 (1997) 171–178.
[40] Y. Lavrovsky, S. Chen, A.K. Roy, Therapeutic potential and mechanism of action of oligonucleotides and ribozymes, Biochem. Mol. Med. 62 (1997) 11–22.
[41] J. Minchull, T. Hunt, The use of single stranded DNA and RNase H to promote quantitative 'hybrid arrest of translation' of mRNA/DNA hybrids in reticulocyte lysate cell-free translations, Nucleic Acids Res. 14 (1986) 6433–6451.
[42] R.Y. Walder, J.A. Walder, Role of RNase H in hybrid-arrested translation by antisense oligonucleotides, Proc. Natl. Acad. Sci. USA 85 (1988) 5011–5015.
[43] R.V. Giles, D.G. Spiller, D.M. Tidd, Detection of ribonuclease H-generated mRNA fragments in human leukemia cells following reversible membrane permeabilization in the presence of antisense oligodeoxynucleotides, Antisense Res. Dev. 5 (1995) 23–31.
[44] Y. Sawai, N. Kitahara, W.L. Thung, M. Yanokura, K. Tsukada, Nuclear location of ribonuclease H and increased level of magnesium-dependent ribonuclease H in rat liver on thioacetamide treatment, J. Biochem. 90 (1981) 11–16.
[45] G.J. Veal, S. Agrawal, R.A. Byrn, Sequence-specific RNase H cleavage of *gag* mRNA from HIV-1 infected cells by an antisense oligonucleotide in vitro, Nucleic Acids Res. 26 (1998) 5670–5675.
[46] E. Uhlmann, A. Peyman, Antisense oligonucleotides: a new therapeutic principle, Chem. Rev. 90 (1990) 543–584.
[47] T. Kanamaru, T. Takagi, Y. Takakura, M. Hashida, Biological effects and cellular uptake of c-myc antisense oligonucleotides and their cationic liposome complexes, J. Drug Targeting 5 (1998) 235–246.
[48] A. Noguchi, T. Furuno, C. Kawaura, M. Nakanishi, Membrane fusion plays an important role in gene transfection mediated by cationic liposomes, FEBS Lett. 433 (1998) 169–173.
[49] O. Zelphati, L.S. Uyechi, L.G. Barron, F.C. Szoka Jr., Effect of serum components on the physico-chemical properties of cationic lipid/oligonucleotide complexed and on their interactions with cells, Biochim. Biophys. Acta 1390 (1998) 119–133.